Zebrafish larvae locomotion bioassay: application on nanofractionated Naja nigricollis venom

Calderoni, G.; Xu, H.; Nelck, H.; Slagboom, J.; Richardson, M.K.; Kool, J.; Tudorache, C.

Taylor & Francis
Taylor & Francis Group

Toxicology Mechanisms and Methods

ISSN: 1537-6516 (Print) 1537-6524 (Online) Journal homepage: www.tandfonline.com/journals/itxm20

Zebrafish larvae locomotion bioassay: application on nanofractionated *Naja nigricollis* venom

Gregorio Calderoni, Haifeng Xu, Hugo Nelck, Julien Slagboom, Michael K. Richardson, Jeroen Kool & Christian Tudorache

To cite this article: Gregorio Calderoni, Haifeng Xu, Hugo Nelck, Julien Slagboom, Michael K. Richardson, Jeroen Kool & Christian Tudorache (2025) Zebrafish larvae locomotion bioassay: application on nanofractionated *Naja nigricollis* venom, Toxicology Mechanisms and Methods, 35:8, 1057-1073, DOI: 10.1080/15376516.2025.2509740

To link to this article: https://doi.org/10.1080/15376516.2025.2509740

TOXICOLOGY MECHANISMS AND METHODS
2025, VOL. 35, NO. 8, 1057–1073
https://doi.org/10.1080/15376516.2025.2509740

Taylor & Francis
Taylor & Francis Group

RESEARCH ARTICLE

OPEN ACCESS Check for updates

Zebrafish larvae locomotion bioassay: application on nanofractionated *Naja nigricollis* venom

Gregorio Calderoni[a,b], Haifeng Xu[b,c], Hugo Nelck[a,b], Julien Slagboom[b,c], Michael K. Richardson[a], Jeroen Kool[b,c#] and Christian Tudorache[a#]

[a]Institute of Biology, University of Leiden, Leiden, the Netherlands; [b]Division of BioAnalytical Chemistry, Department of Chemistry and Pharmaceutical Sciences, Amsterdam Institute of Molecular and Life Sciences, Vrije Universiteit Amsterdam, Amsterdam, the Netherlands; [c]Centre for Analytical Sciences Amsterdam (CASA), Amsterdam, the Netherlands

ABSTRACT

Snakebite envenoming remains a major global health issue, particularly in underserved regions. To better understand venom composition and toxic effects, crude snake venoms can be fractionated into distinct toxin groups using high-throughput nanofractionation analytics. These fractions can then be assessed using venomics to identify specific toxins, in conjunction with bioassays to evaluate their bioactivity. Traditional *in vivo* testing in rodents is limited by legal and ethical concerns, the high number of fractions, and the small quantities of toxins in each. In this study, zebrafish larvae were introduced as an efficient alternative model for *in vivo* analysis of toxins that impair locomotion. A behavioral bioassay was developed using a light-dark challenge to assess locomotion in 5-day post-fertilization (dpf) larvae. A Locomotion Index was created to compare movement during the dark phase between venom-exposed and control groups. Using venom from the spitting cobra *Naja nigricollis*, two fractions were found to reduce locomotor activity significantly. Microscopic screening also revealed three tissue-toxic fractions, one of which caused bradycardia. Dose-response testing was performed for each toxic fraction. Furthermore, oxygen consumption assays were conducted with venom fractions from *N. nigricollis, N.haje, N. siamensis,* and *N. subfulva*, identifying two fractions that elevated oxygen consumption. High-throughput venomics linked these toxic effects to three-finger toxins and phospholipases A_2. This integrative approach offers a scalable, efficient method for *in vivo* toxicity screening of venom components and shows promise for broader applications in the discovery and profiling of diverse bioactive compounds.

ARTICLE HISTORY
Received 27 March 2025
Revised 16 May 2025
Accepted 16 May 2025

KEYWORDS
Snake venom; nanofractionation; zebrafish; bioassay; neurotoxicity; cytotoxicity; tissue toxicity; light-dark challenge; *Naja nigricollis*

Introduction

Snakebite in humans is a high priority Neglected Tropical Disease, according to the World Health Organization (2018). As many as 81,410–137,880 people die each year worldwide from snakebite (Chippaux 1998; Kasturiratne et al. 2008). Further, more than 400,000 people per year are left with life-long disabilities due to complications from snakebite envenoming (Gutiérrez et al. 2017). The harmful effects of snake venoms are due to their constituent toxins, which encompass at least 63 different protein families, including PLA2, SVMP, SVSP and 3FTx as dominant, and KUN, CRiSP, LAAO, CTL, DIS, and NP as secondary families, with PLA2s and 3FTX being the most abundant toxin families in the venoms of most elapid snakes (Tasoulis and Isbister 2017). Several evolutionary mechanisms have been proposed to explain the complex composition of snake venoms. According to one hypothesis there is a coevolutionary arms-race between venomous snakes and their preys, in which the prey evolves resistance to the toxins, and the snake evolves novel toxic means to overcome the prey resistance (Bucciarelli et al. 2022; van Thiel et al. 2022). This adaptive process explains why some snake venoms pose such a deadly threat to humans, who play no role in these snakes' evolutionary arms race: there is no strong selective pressure being exerted on humans by venomous

CONTACT Jeroen Kool j.kool@vu.nl Division of BioAnalytical Chemistry, Department of Chemistry and Pharmaceutical Sciences, Amsterdam Institute of Molecular and Life Sciences, Vrije Universiteit Amsterdam, Amsterdam, the Netherlands; Christian Tudorache c.tudorache@biology.leidenuniv.nl Institute of Biology, University of Leiden, Leiden, the Netherlands
[#]Equally contributing authors

Supplemental data for this article can be accessed online at https://doi.org/10.1080/15376516.2025.2509740.

snakes, thus leaving us with less tools to fight off snake toxins (Casewell et al. 2020).

A recently developed method in venomics known as nanofractionation is able to process crude snake venoms for chemical and biochemical assessment of their toxins (Slagboom et al. 2020; Xie et al. 2021). It consists of performing a liquid chromatography separation of crude venom, followed by high resolution nanofractionation onto plate reader well plates and parallel mass spectrometry detection, subdividing groups of toxins in a large number of separate nanofractions. After this, the next step is to characterize specific toxins within each nanofraction both chemically and in terms of bioactivity. To identify the toxins in each fraction, high-throughput (HT) venomics as established by Slagboom et al. (2023) can be applied. In brief, tryptic digests of each fraction undergo proteomics analysis, and the protein scores for each toxin found in each fraction are plotted on the y-axis versus fractionation retention time (RT) on the x-axis, thereby producing for each toxin so-called protein score chromatograms (PSCs). This nanofractionation analytics methodology allows a relatively rapid profiling of multiple venoms.

A large array of *in vitro* bioassays has been implemented into the nanofractionation approach (Mladic et al. 2016, 2017, 2018; Otvos et al. 2016; Still et al. 2017, 2020; Zietek et al. 2018; Neumann et al. 2020; Xie et al. 2021, 2020; Arrahman et al. 2022; Bittenbinder et al. 2023). *In vivo* bioassaying of collected fractions using murine models with this analytical approach is practically impossible because of the large numbers of fractions collected, the low amounts of toxin in each fraction, the high cost of husbandry, and legal ethical issues arising from the large number of experimental animals needed.

An alternative to using murine models in bioassays is to use the zebrafish (*Danio rerio*). The zebrafish can be used to model the effect of toxins on mammals (Legradi et al. 2015; Vargas et al. 2015; Bauer et al. 2021), and various types of organ-specific toxicity can be assayed (Peterson and MacRae 2012; Dai et al. 2014; Horzmann and Freeman 2018; Cassar et al. 2020). Furthermore, the zebrafish has previously been used to screen and analyze crude snake venoms (Carvalho et al. 2018; Zanotty et al. 2019; Sahyoun et al. 2022). While a complete substitution of more complex model organisms is not yet feasible (Tal et al. 2020), the zebrafish model is proving to be a valuable alternative thanks to its much lower costs, high-throughput, and legal ethical benefits its embryos and larvae provide (Howe et al. 2013; Bressan Simonetti et al. 2016; Canedo et al. 2022).

In addition to its use in toxicology screening, the zebrafish model can be used in behavioral research. Different tests combined with software analysis can allow numerous kinematic parameters and behavioral responses to be measured and analyzed, even during early larval stages (Moretz et al. 2007; Champagne et al. 2010; de Esch et al. 2012; Wong et al. 2012; Legradi et al. 2015; Tudorache et al. 2015; Basnet et al. 2019; Grieco et al. 2020). One behavioral test, the light-dark challenge (LDC), allows anxiety-like responses in zebrafish and mammals to be recorded. It is based on the tendency of these animals to be alarmed by darkness (Steenbergen et al. 2011). After an acclimatization period where larvae reach a baseline level of locomotion, a sudden alternation of light and dark conditions induces, respectively, hypoactivity (freezing behavior) and hyperactivity in the subjects compared to the baseline (Emran et al. 2008; Ellis et al. 2012; Peng et al. 2016; Luchtenburg et al. 2019; Faught and Vijayan 2022).

Our research focus is on the effect of snake toxins on locomotion. Snake toxins have a variety of mechanisms of action affecting the locomotion of an organism. Among them, three-finger toxins (3FTX), the most abundant toxin family in the venoms of elapid snakes (Tasoulis and Isbister 2017), are mainly responsible for the neurotoxic properties of their venoms (Ranawaka et al. 2013). In particular, α-neurotoxins compete with acetylcholine for binding to the nicotinic acetylcholine receptors on post-synaptic membrane of the neuromuscular junction, leading to flaccid paralysis of skeletal muscle (Barber et al. 2013; Ranawaka et al. 2013; Dutta et al. 2017). Flaccid paralysis of skeletal muscles–which in severe cases can cause death by respiratory failure after blocking respiratory muscles in mammals (Gutiérrez et al. 2017)–is also achieved by β-neurotoxins, which enzymatically hydrolyze phospholipidic membranes at the presynaptic side of the neuromuscular junction (Pungerčar and Križaj 2007). β-neurotoxins belong to the phospholipases A_2 (PLA_2) family (Mackessy 2009; Adamude et al. 2021). Indeed, different toxins can affect the neuromuscular junction acting on various cellular structures and molecules, and more can alter locomotion in the subject as a direct or indirect consequence of their toxic action. For example, myotoxins can directly affect locomotion by killing skeletal muscle cells, whereas cardiotoxins and haemotoxins can disrupt haemodynamics, or debilitating hemorrhagic toxins and pain-inducing toxins may cause paralysis (Warrell 2010; Gutiérrez et al. 2017), indirectly leading to locomotion alterations.

In this study, a behavioral assay using zebrafish larvae as a whole-organism vertebrate model was integrated within nanofractionation analytics. We used this

approach to rapidly study the effects on locomotion of toxins isolated from snake venoms, developing a high-throughput method for profiling toxicity types, and measuring the potency of toxin bioactivities. The present study is a proof-of-concept of our approach. The venom of the black-necked spitting cobra (*Naja nigricollis*) was chosen because of its known neurotoxic and cytotoxic venom composition (Adamude et al. 2021). The analytical approach with integrated *in vivo* behavioral and toxicity profiling workflow is summarized in Figure 1.

Materials and methods

Venom

Lyophilized snake venom from four cobra species (*Naja haje*, *Naja nigricollis*, *Naja siamensis*, and *Naja subfulva*) was provided by the Center for Snakebite Research and Interventions Herpetarium (Liverpool School of Tropical Medicine, United Kingdom). The lyophilized venom was stored long-term at −80 °C. A stock solution of crude venom (2.5 ± 0.1 mg/mL) was prepared in MilliQ water before analysis, and then aliquoted and stored at −80 °C until use. Ultrapure water (named MilliQ water in this study) was produced *via* a MilliQ system.

RP-HPLC separation, nanofractionation, and mass spectrometry

50 µL of 2.5 mg/mL venom solution was injected by a Shimadzu SIL-20AC autosampler and then separated on a 100 × 4.6 mm ID analytical column packed with Xbridge BEH300 reversed-phase C18 material (3.5-µm particle size) at 30 °C in a Shimadzu CTD-10AC column oven. The elute with a total flow rate of 0.5 mL/min, controlled by a Shimadzu LC-20AB parallel A, B pump, was first sent to a Shimadzu SPD 20 A UV-Vis detector (220 nm). The gradient used consisted of a linear increase of the mobile phase B from 0% to 10% performed in 10 min, followed by going from 10% to 95% in 20 min. The steepness of the gradient was chosen to reduce the number of peaks to be further tested in the zebrafish bioassay. Less steep gradients would have resulted in slightly better separations, but also in broader peaks. After 2 min, a decrease from 95% to 0% B in 7 min with equilibration for 2 min was carried out. Mobile phase A was water-acetonitrile-trifluoroacetic acid (98:2:0.1, v/v/v), and mobile phase B was water-acetonitrile-trifluoroacetic acid (2:98:0.1, v/v/v).

After UV detection, 90% of the fraction was transferred to a FractioMate™ FRM100 nanofractionation collector (Vrije Universiteit, Amsterdam, The Netherlands)

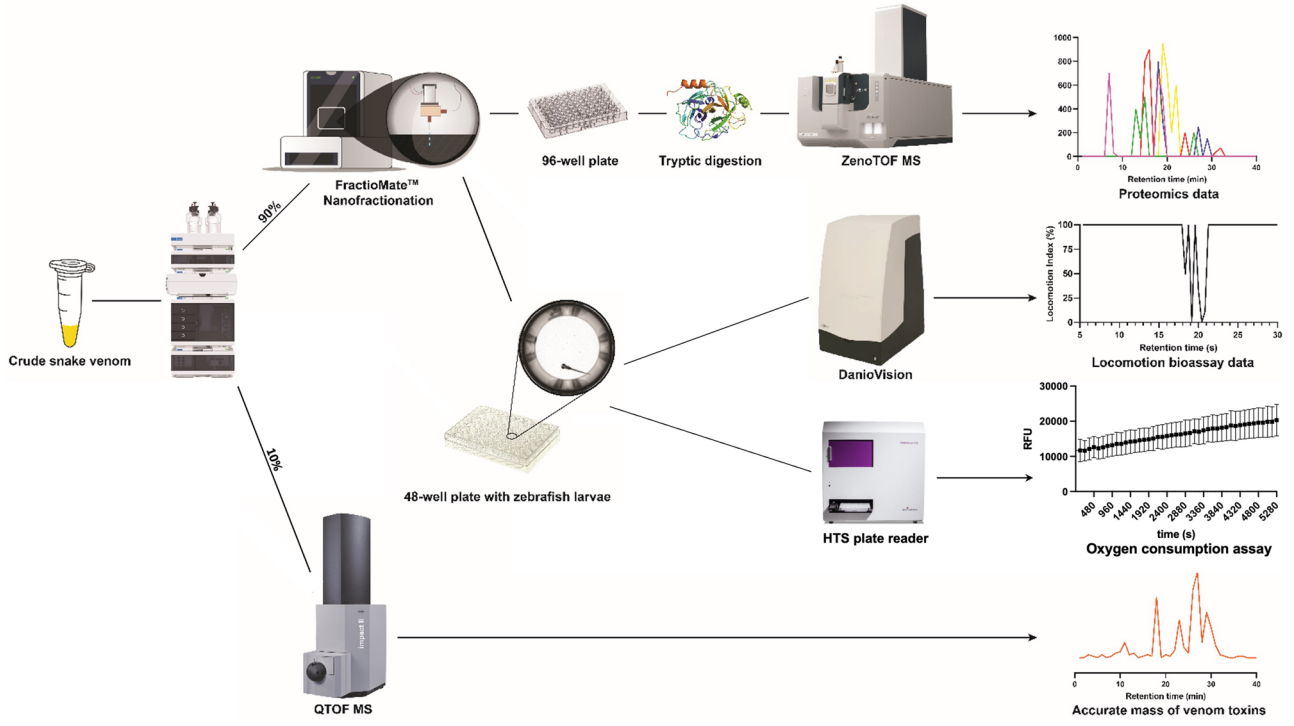

Figure 1. Schematic overview of the locomotion bioassay and toxicity profiling workflow. Crude snake venom is separated by RP-HPLC: 10% of the elute goes through online intact MS measurement, while 90% is collected by a FractioMate at 25 s per well in a 96-well plate. After vacuum-centrifuge drying, the plates separately undergo toxin identification by HT venomics following tryptic digestion, *in vivo* locomotion bioassaying, using DanioVision to track the movements of zebrafish larvae in a 48-well plate while running a light-dark challenge, and oxygen consumption measurement in real time.

controlled by FractioMator software. The fractions were collected at a resolution of 25 s per well into 96-well plates (F-bottom, rounded square well, polystyrene, without lid, clear, non-sterile; Greiner Bio One, Alphen aan den Rijn, The Netherlands) with a 5 min delay between injection and start of the fractionation process. Well plates with collected fractions were subsequently vacuum-centrifuged to dryness overnight using a Christ Rotational Vacuum Concentrator (RVC 2–33CD plus, Zalm en Kipp, Breukelen, The Netherlands) operated with *a* − 80 °C cooling trap. The dried plates were stored at −20 °C until bioassaying or HT venomics.

The remaining 10% of the elute was sent to MS detection (IMPACT II QTOF, Bruker Daltonics, Germany) operated with electrospray ionization (ESI) in positive-ion mode in the range between 800 and 5500 *m/z*. The ESI source parameters were a capillary voltage of 3.5 kV, source temperature of 200 °C, nebulizer at 0.8 Bar, and dry gas flow at 6.0 L/min. Collision-induced dissociation (CID) was set at 200 eV, and 1 average spectrum was stored per s. Bruker Compass software was used for instrument control and data analysis.

For MS data processing, total-ion current (TIC) was plotted from the recorded MS. Extracted-ion currents (XICs) were extracted from TIC with *m/z* value, accurate mass data, and charge status. By matching with the bioactivity chromatogram through RT and peak shape, those XICs were likely assigned as bioactive accurate masses of the bioactive toxins. Bruker Compass Data Analysis software was used for instrument control and data analysis.

Due to small time differences of eluted toxins for arriving at UV and at MS detection, and for fractionation, the UV, MS and fractionation times need to be aligned. This was done by measuring the RT of thrombin inhibitor argatroban in UV and MS, and by fractionating the inhibitor on a well plate followed by performing a coagulation bioassay as described by Slagboom et al. (2020). The bioassay chromatogram resulting from the coagulation bioassay gives a negative peak for argatroban from which an RT can be measured. By measuring the differences in RT between UV, MS, and the coagulation bioassay, the delay times were calculated and used to align the UV, MS, and bioassay data presented in this study.

High-throughput venomics

HT venomics was developed by Slagboom et al. (2023) and applied in this study. Nanofractionated venom toxins in the wells obtained through nanofractionation were mixed with 25 µL of 25 mM ammonium bicarbonate and 0.05% β-mercaptoethanol (pH 8.2) and heated at 95 °C for 15 min for the reduction step. Then, after cooling the well plate to room temperature 10 µL 12.5 mM Iodoacetamide was added and incubated for 30 min at room temperature in the dark for alkylation. Next, a trypsin solution was made from a stock solution (1 µg/µL trypsin in 50 mM acetic acid) by diluting the stock 100 times in 25 mM ammonium bicarbonate. Then, 10 µL trypsin solution was added to each well and the plates were incubated overnight at 37 °C. Next, the plates were centrifuged at 1000 rpm for 1 min in an Eppendorf Centrifuge 5810 R followed by the addition of 10 µL of 1.25% formic acid to the wells. Finally, the plates were analyzed using nanoLC − MS/MS. For this, the digested samples were separated by an UltiMate 3000RSLCnano system (Thermo Fisher Scientific, Ermelo, The Netherlands) with an Acclaim PepMap 100 C18 HPLC Column (150 mm × 75 µm, 2 µm particle size, 100 Å pores) in combination with an Acclaim PepMap 100 C18 trapping column (5 mm × 0.3 mm, 5 µm particle size, 100 Å pores, Thermo Fisher Scientific). The columns were kept in a column oven at 45 °C. The autosampler was run in full-loop injection mode with a 1 µL injection volume. Mobile phase A consisted of 98% H_2O, 2% ACN, and 0.1% FA and mobile phase B was 98% ACN, 2% H_2O, and 0.1% FA. The gradient started with a 3 min isocratic separation at 1% B, then a linear increase to 40% B in 7.5 min followed by a linear increase to 85% B in 0.1 min, 0.7 min isocratic separation at 85% B, linear decrease to 1% B in 0.2 min, and equilibration at 1% B for 3.7 min. Detection was done by a Bruker maXis II qTOF mass spectrometer (Bruker Daltonics, Germany) equipped with a Bruker Captivespray source operating in positive-ion mode. The source parameters were: source temperature, 150 °C; capillary voltage, 1.2 kV; gas flow, 3 L/min. Spectral data were acquired at a rate of 1 average spectrum/s in the range of 50 to 3000 *m/z*. MS/MS spectra were obtained using collision-induced dissociation (CID) in data-dependent mode using 10-eV collision energy. Bruker Compass software version 3.0 was used for instrument control and data analysis. Mascot mgf files were generated by using the ProcessWithMethod function from the results of each well. These files allow subsequent Mascot (Matrix Science, London, United Kingdom) database searches which were done using the UniProt database searching under Serpentes accessions only. R packages (R Core Team 2022) were used for processing the Mascot results in a high-throughput fashion resulting in an Excel document with UniProt retrieved information (such as toxin family, toxin name, toxin accession code, protein score, sequence coverage) for each well. The HT venomics data were finally plotted as PSCs according to Slagboom et al. (2023) for which, for each toxin ID found in each well, its

corresponding protein score was plotted on the y-axis versus RT of fractionation of each well from which the result was derived on the x-axis. The venomics data are available in the Supporting Information.

Zebrafish husbandry

Zebrafish were handled in compliance with the directives of the local animal welfare committee of Leiden University and maintained according to standard protocols (zfin.org). All protocols adhered to the international guidelines specified by the EU Animal Protection Directive 2010/63/EU. Adult wild-type zebrafish (ABTL strain) were housed and reared under standard Leiden University facility conditions at a constant temperature of 28.5 ± 0.5 °C in densities of 30 to 33 individuals (male:female ~ 1:1) in 7.5 L tanks in standardized recirculation systems (Fleuren and Nooijen; Nederweert, The Netherlands). Ambient light conditions (i.e. 0–425 ± 11 ln m^{-2} with 15 min dusk and dawn period) were maintained as 14:10 h day:night cycles, with light periods from 08:00 am to 10:00 pm. Temperature and light conditions are based on standard summer conditions in South Asia, the original geographic range of *D. rerio* (Engeszer et al. 2007). Fish were fed twice a day with dry food (DuplaRinM; Gelsdorf, Germany) and frozen artemia (Dutch Select Food, Aquadistri BV; Klundert, The Netherlands).

Between 3 pm and 6 pm, adults from one 7.5 L tank were divided into 3 sloping breeding tanks. The following morning between 9 am and 12 pm the fish were put back in the 7.5 L tank, and the eggs were harvested with a sieve and placed in a 50 mL tube filled with egg water (60 mg/mL "Instant Ocean" sea salts, Aquarium Systems, Blacksburg, USA, in MilliQ water with 2 drops of methylene blue per 100 mL). From this step onwards, the eggs were transferred to a different facility where they were kept at 29 °C where a 12:12 h day:night cycle was in use. Around 80 eggs were then placed in a 90 mm Petri dish containing fresh egg water. This egg water was used throughout the experimentation. After 1–2 days the unfertilized eggs were removed, and the Petri dishes replenished with fresh egg water. All experiments were performed at 5 days post-fertilisation (dpf).

Ethics statement

According to the European legislation on animal experimentation as implemented by the Dutch government (WOD), zebrafish larvae up to 6 dpf are not considered experimental animals and are therefore exempt from Animal Welfare regulations. Approval from the ethics committee of Leiden University is therefore not applicable.

Venom plate preparation and fish handling

The optimal concentration of 2.5 mg/mL crude venom was determined by range-finding (data not shown), with an injection volume for the chromatographic separation of 50 µL. Moreover, the bioactive range of toxins was narrowed down within 10 subsequent fractions of the 96-well plate, which were tested in all experiments. 180 µL of egg water was added to the wells of the 96-well plate with the freeze-dried venom fractions, and initial fraction solutions obtained were mixed and left to rest for 10 min. The following volumes of initial fraction solutions were diluted: 50 µL, 47 µL, 44 µL, 37.5 µL, 25 µL, 12.5 µL, and 0 µL (negative controls). Each initial fraction solution was pipetted into a new 96-well plate, followed by adding 250 µL minus the initial fraction solution volume of egg water and gently mixing. The zebrafish larvae were transferred to a 48-well plate by pipetting 250 µL of egg water and one larva in each well. To avoid injuring the larvae, we used a 1000 µL pipette tip whose opening was widened by cutting its extremity. Before testing, an acclimatization period of 20 min was applied to let the fish recover from handling. Then, each of the resulting 250 µL fraction solutions was transferred from the 96-well plate to the 48-well plate containing the larvae in 250 µL of egg water, obtaining the final concentrations of 10%, 9.4%, 8.8%, 7.5%, 5%, and 2.5% (v/v), respectively. The light-dark challenge began immediately afterwards.

For the oxygen consumption test, two 96-well lyophilized venom plates were prepared for each crude venom sample of *N. haje* (Nha), *N. nigricollis* (Nni), *N. siamensis* (Nsi) and *N. subfulva* (Nsu), to establish triplicates for all fractions. These were realized by reconstituting the lyophilized venom fractions with 100 µL of egg water per well and left to rest for ca 10 min. Then, for each 96-well lyophilized venom plate, three new plates were prepared, each well containing 100 µL of egg water and a single zebrafish larva. Subsequently, 50 µL of the reconstituted venom fraction was transferred to the corresponding wells containing larvae. After administering the reconstituted venom to the larvae, the plates were left to rest for one hour before assessing toxicity effects.

Light-dark challenge assay

For the light-dark challenge assay, 5 dpf larvae were subjected to short alternating periods of light and darkness to elicit an anxiety-like response, and their movements in response to these stimuli were recorded. The 48-well plate with one zebrafish larva per well

was placed in a DanioVision™ observation chamber (Noldus Inc., Wageningen, The Netherlands), equipped with infrared lighting underneath the plate and an infrared-sensitive camera filming from above (30 fps; 1280 × 960 pixels). After 30 min of acclimatization in the light, returning baseline locomotion values, the animals were exposed to a 7.5 min challenge phase in the dark eliciting a hyperactive locomotion response, followed by another 7.5 min challenge phase in the light, eliciting a hypoactive response in comparison to baseline activity. This cycle of dark and light challenge phases was repeated twice, resulting in four alternating dark and light phases that lasted 30 min in total. The plate arena was adapted to the brand and model of the 48-well plates used and the volume of solution in the wells (500 µL). A low-pass filter of 0.4 mm was applied, deleting every shorter movement detected by the software. This number was produced by running a test on dead larvae and selecting the lowest number that would give no movement results. Tracking the movement of the larvae and analyzing the resulting behavioral data was carried out using EthoVision XT software (Version 14.0; Noldus, Wageningen, The Netherlands). The total distance moved (D, mm) was recorded for each animal to obtain locomotor activity data (Tudorache et al. 2015; Rock et al. 2022).

Lethality and toxicity screening

After each experimental trial, all larvae exposed to 10% (v/v) fractions were checked to confirm their survival and the toxicity type of the fractions. This was done by attempting to trigger the fish touch response by nudging each larva with a Pasteur pipette. The larvae which did not respond to this stimulus were inspected under a stereomicroscope and categorized as alive (heart beating) or dead (no heartbeat). Tissue toxicity was then assessed through visual confirmation of local tissue damage. Full paralysis was confirmed when a live larva did not show a touch response and had no visible tissue damage. For the heart rate counts, the larvae were immobilized using the anesthetic MS-222 (Finquel, Argent Chemical Laboratories; Redmond, USA) at 168 mg per liter of egg water (Leyden et al. 2022), after buffering the solution with the same amount of sodium carbonate. The number of heart beats per minute was counted 30 min after exposure to the fractions and MS-222. Each larva was placed under a stereomicroscope and the heartbeats visually counted for 1 min. To avoid damaging the larvae, they were transferred using Pasteur pipettes that had their openings cut wider.

Locomotion Index

In order to return results in a comprehensive way, we introduced the Locomotion Index (LI; in %). To calculate the LI, the following process was adopted: for each experimental trial, the raw data of D (mm; generated in EthoVision) were analyzed for outliers (Q ROUT = 10%), which were subsequently removed, and an average over 30 s was created. Then, these values were used to create an average D ± SD of the two dark phases (D_{dark}), and an average D ± SD of all the controls in the trial (D_{contr}). For each venom fraction in each trial, a ratio was calculated by dividing D_{dark} by D_{contr}. Then, each data point was multiplied by 100, making the resulting index a percentage. A LI higher than the control baseline (100%) is considered to represent hyperactivity, and one lower than the baseline represents hypoactivity, as compared to non-treated controls. The aforementioned data processing was carried out by writing and running original *ad hoc* scripts for the programming language R (R Core Team 2022), using the integrated development environment RStudio (RStudio Team 2022). The script is available in the Supporting Information, Script 1.

Oxygen consumption

For the estimation of the effect of venom fractions on the metabolic rate in living zebrafish larvae, an oxygen consumption assay was performed using an Agilent MitoXpress Xtra oxygen consumption assay kit (Agilent Technologies, Santa Clara, USA), which allows real-time measurement of extracellular oxygen consumption in a living organism. Here we tested another possible bioassay to quantify a different physiological measurement, showcasing the range of different tests that can easily be made *in vivo* on the zebrafish larvae. First, 180 µL of egg water was added to the wells of the 96-well plate containing freeze-dried venom (fractions Nsi_F7 at 23 min, Nha_D12 at 35.6 min, Nni_H6 at 21 min, Nni_G1 at 7.3 min and Nsu_H12 at 37 min) to make the stock solution and left to rest for 10 min. Then, 80 µL egg water containing a single larva was pipetted into each well of a 96-well plate (Cellstar, Dallas, USA). To prevent injuring the larvae, the opening of the pipette tip was widened by cutting off its end. After that, 10 µL was pipetted to the wells containing a larva. Using a multi-pipette, 10 µL MitoXpress Xtra was added to each of the wells. Finally, all wells were sealed quickly with two drops of preheated (28 °C) Agilent HS Mineral Oil to isolate the medium from exterior oxygen. The plate was then transferred

to a Tecan Spark M20 spectrofluorometer, previously preheated to 28 °C, and pre-set to an excitation wavelength of 380 nm and an emission wavelength of 650 nm. The plate-reader measured the fluorescence every two minutes over a period of 90 min. The positive control consisted of 90 µL eggwater and 10 µL MitoXpress Xtra per each larva containing a well, blank measurements were performed with the same concentration but without larvae. Only fractions showing sublethal effects were used for data analysis.

Data analysis

The data from 10% fractions (Figure 2) were tested for statistical significance by performing a one sample t-test on the LI of treatments against the LI baseline (100%), producing p-values for each treatment. The heart rate data (Figure 3) were tested for significance by performing Brown-Forsythe and Welch's ANOVA tests, followed up by Dunnett's T3 multiple comparisons test comparing the treatments against the control group, producing *p* values for each treatment. Oxygen consumption, as fluorescence change rate in relative fluorescence units (RFU) over time, was tested for significance by first subtracting blank values from measurements over time, removing outliers (ROUT $Q = 10\%$), and then performing a simple linear regression analysis, with the resulting slopes being compared using a Brown-Forsythe and Welch's ANOVA with a Dunnett's T3 multiple comparisons test (Figure 4).

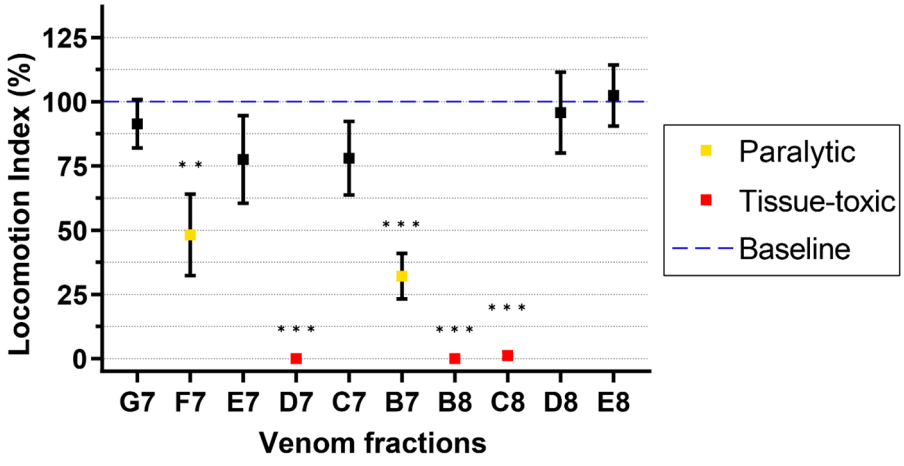

Figure 2. Average LI of 10% (v/v) *Naja nigricollis* venom fractions G7, F7, E7, D7, C7, B7, B8, C8, D8, and E8 (17.9, 18.3, 18.75, 19.2, 19.6, 20, 20.4, 20.8, 21.3, 21.7 min RT, respectively). All values are presented as mean ± SEM. One sample t-test against the baseline (100%). $n = 12$, B8 and E8 $n = 10$. $^{**}p < 0.01$, $^{***}p < 0.001$.

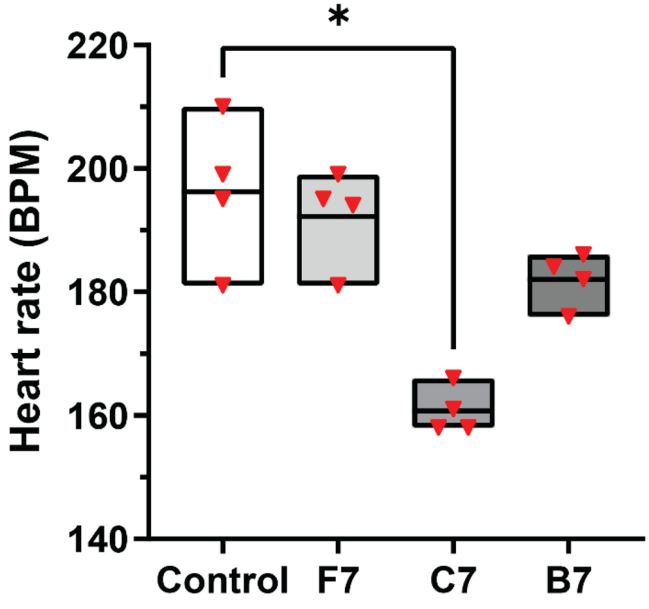

Figure 3. Heart rate of larvae after 30 min exposure to 10% (v/v) *Naja nigricollis* venom fractions F7, C7, B7 (18.3, 19.6, 20 min RT respectively), and 168 mg/L MS-222. Line at mean, data points shown. Brown-forsythe and welch's ANOVA tests, followed up by dunnett's T3 multiple comparisons test comparing treatments against the control group. $^{*}p < 0.05$. $n = 4$.

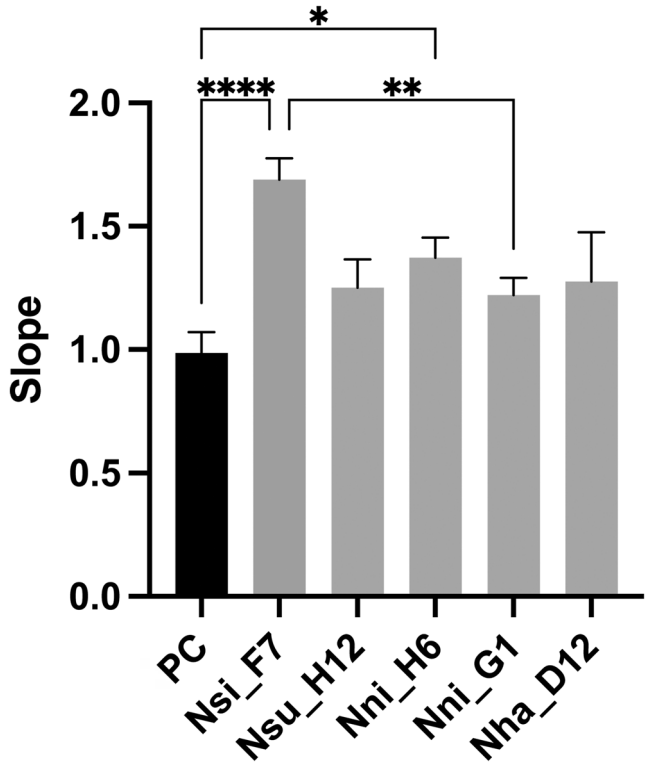

Figure 4. Oxygen consumption as slopes of RFU values over 90 min for the fractions tested. Brown-forsythe and welch's ANOVA tests, followed up by dunnett's T3 multiple comparisons test comparing treatments against the control group. *$p < 0.05$, ** $p < 0.01$, **** $p < 0.0001$. $n = 15$.

Data analysis and inferential statistics were performed using GraphPad Prism (Version 9.5.1, GraphPad, Boston, USA). Figures were processed using Adobe Photoshop and Adobe Illustrator (Adobe, San Jose, USA).

Results

Fractions bioactivity graph

10% *N. nigricollis* fractions were tested using our zebrafish larvae locomotion bioassay protocol, and the average LI for each fraction was measured (Figure 2). Fractions F7 (18.3 min RT) and B7 (20 min RT) showed an average LI of 48% ($p < 0.01$) and 32% ($p < 0.001$) respectively, and were identified as paralytic. Fractions D7 (19.2 min RT), B8 (20.4 min RT) and C8 (20.8 min RT) showed an average LI of 0%, 0% and 1% respectively ($p < 0.001$), and were identified as tissue-toxic.

Fractions dose-response curves

The same bioassay experiment used to obtain the fractions bioactivity graph for the 10% fractions (Figure 2) was performed for the significantly toxic fractions (i.e. F7, D7, B7, B8, and C8) using different dilutions, namely 2.5%, 5%, 7.5%, 8.8%, and 9.4% (v/v). Data for 10% fractions were also used in Figure 5. A variable slope was fitted for each bioactive fraction result using least squares regression, showing the specific dose-response profiles (Figure 5). Paralytic fraction F7 showed a relatively linear descending curve, whereas fractions B7, D7, B8, and C8 exhibited very steep descending curves after a certain concentration. Based on our results, the LD_{100} of D7 and B8 was at 5% (actual range: 2.5% < $LD_{100} \leq 5\%$), whereas C8 had its LD_{100} at 9.4% (actual range: 8.8% < $LD_{100} \leq 9.4\%$).

Lethality and toxicity screening

After zebrafish larvae were exposed to 10% (v/v) fractions, fractions F7 and B7 were both lethal to 2/12 larvae (16.7%), whereas fractions D7, B8, and C8 were lethal for 12/12 (100%) each (Figure 2). Fractions F7 and B7 were paralytic, with F7 causing full paralysis in 2/12 larvae (16.7%) and B7 in 3/12 (25%). Tissue toxicity as local tissue damage was confirmed for Fractions D7, B8, and C8, all showing similar degrees of tissue toxicity (Figure 6). Following up on the presence of blood pooling in the heart (Supporting Information Fig. S1) of subjects exposed to fraction F7, C7, and B7, the heart rate of subjects

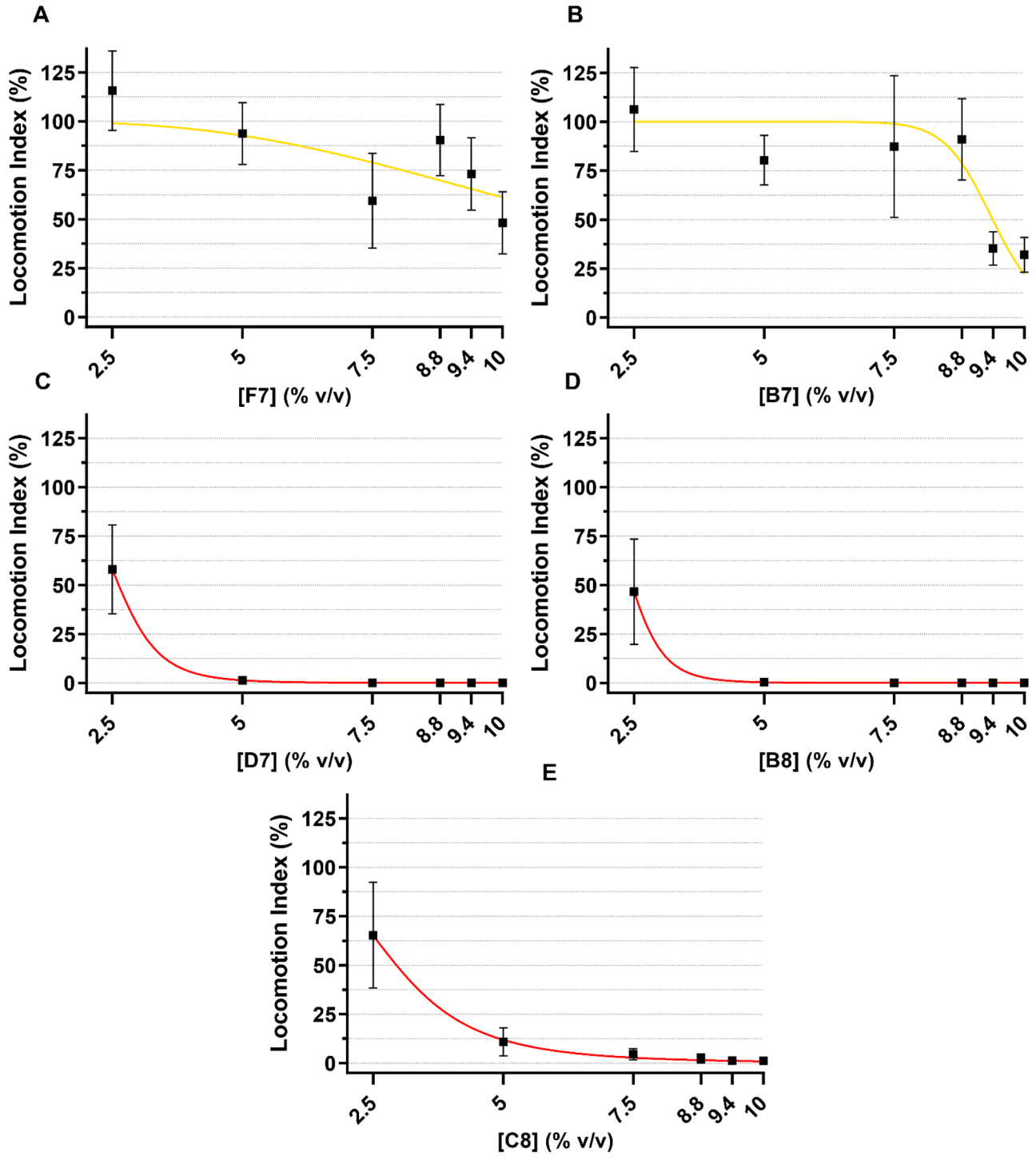

Figure 5. Dose-response curves of *Naja nigricollis* venom fractions. Toxicity type shown (yellow: paralytic; red: tissue-toxic). All values are presented as mean ± SEM. Least squares regression fitting with variable slopes. 2.5%, 5%, and 7.5% $n = 5$; 8.8% and 9.4% $n = 7$; 10% $n = 12$. (A) Fraction F7, 18.3 min RT. $r^2 = 0.57$; (B) Fraction B7, 20 min RT. $r^2 = 0.79$; (C) Fraction D7, 19.2 min RT. $r^2 = 1$; (D) Fraction B8, 20.4 min RT. $r^2 = 1$; (E) Fraction C8, 20.8 min RT. $r^2 = 1$.

exposed to said fractions was measured and compared to a control group after inducing anesthesia to make the counting possible (Figure 3). Only fraction C7 (19.6 min RT)–a fraction which corresponded to a non-significant LI–showed a significantly lower heart rate than the control group ($p < 0.05$).

Oxygen consumption

RFU values over time are presented in Supporting Information, Fig. S3. The slopes of oxygen consumption over time are presented in Figure 4. Brown-Forsythe and Welsh ANOVA with a Dunnett's T3 multiple comparisons test returned a significantly

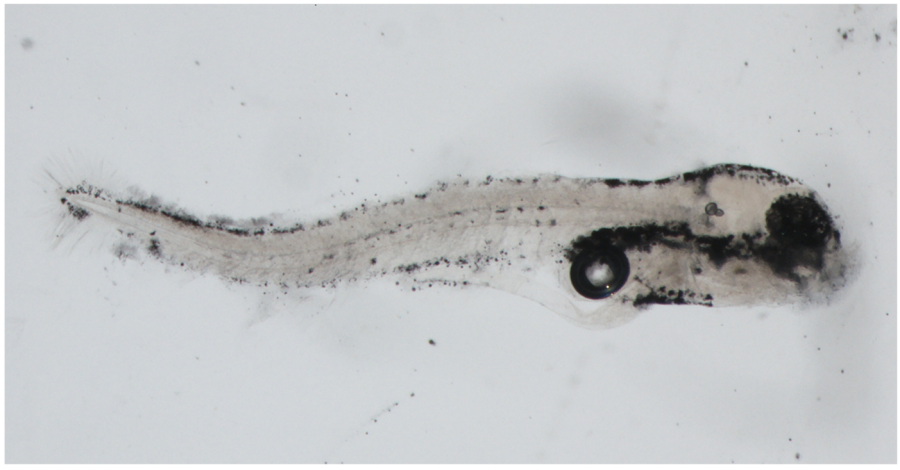

Figure 6. Zebrafish larva showing extensive local tissue damage after 1 h exposure to 10% (v/v) *Naja nigricollis* venom fraction B8 (20.4 min RT).

($p < 0.05$) higher oxygen consumption than non-exposed control for individuals exposed to fractions Nsi_H7 and Nni_H6.

Integrated nanofractionation analytics and toxicity profiling with nanofractions toxins identification by LC-MS and HT venomics

The average LI for all fractions is plotted in bioactivity chromatograms by having on the y-axis the average LI of each fraction at all dilutions *versus* their RT of fractionation on the x-axis. The bioactivity chromatograms are shown in Figure 7E, with the 10% (v/v) producing three negative bioactivity peaks (for the isolated 10% v/v chromatogram, refer to Supporting Information, Fig. S2). Superimposed chromatograms are plotted of the corresponding LC-UV data (Figure 7A), Total Ion Current (TIC; Figure 7B), Extracted Ion Currents (EICs) of toxins eluting at similar RT, peak shape, and RT profiles as one of the negative bioactivity peaks (Figure 7C), and PSCs corresponding to toxin IDs of toxins eluting with similar RT and peak shape profiles as one or more of the negative bioactivity peaks (Figure 6D). The first bioactivity peak was fraction F7, which eluted at 18.3 min and was correlated to one PLA_2 toxin (PA2B4 from Figure 7D) to which a deconvoluted accurate mass of 13245.7 Da (*m/z* value of 2208.8196^{6+}) was tentatively assigned from Figure 7C. The second bioactivity peak (i.e. D7) eluted at 19.2 min and was tentatively correlated to the two toxins 3SAN (Naniproin) and PA2B4 (basic phospholipase A_2). The accurate mass acquired for Naniproin was 6881.4 (*m/z* value of 1722.6109^{4+}). The third bioactivity peak (B7, B8, and C8) eluted from 20 to 20.8 min and was correlated to Nawaprin (WAPN, no matched accurate mass found), basic phospholipase A_2, and Naniproin. This slight deviation from the theoretical monoisotopic mass of the fully oxidized form of Naniproin (6882.47 Da) could be explained by a deamidation of the toxin, which is commonly observed in these types of proteins.

Discussion

In this study, we describe a combined *in vivo* behavioral and energetics bioassay on zebrafish larvae and nanofractionation analytics. We used this implementation to measure toxin-induced locomotion changes in fractions of *N. nigricollis* snake venom, and to identify the toxins responsible. Two fractions were significantly paralytic, and by adding subsequent toxicity screening after the bioassay we were able to identify tissue toxicity in the form of local tissue damage, with three fractions being significantly tissue-toxic. The toxin concentration-hypoactivity correlation was explored for all significantly toxic fractions by fitting dose-response curves. Finally, three fractions induced altered haemodynamics in the subjects with one fraction causing significant bradycardia.

A few choices were made to optimize the bioassay protocol and data processing. We used 48-well plates during the light dark challenge (LDC) assay instead of 96-well plates because the smaller wells of the latter restrain the locomotion of the larvae (Davis et al. 2021). Moreover, instead of using the raw total distance moved (D) data from all phases of the LDC, namely the acclimatization period and the two light and dark challenges, only the two dark phases were analyzed, since the acclimatization phase is highly variable between individuals

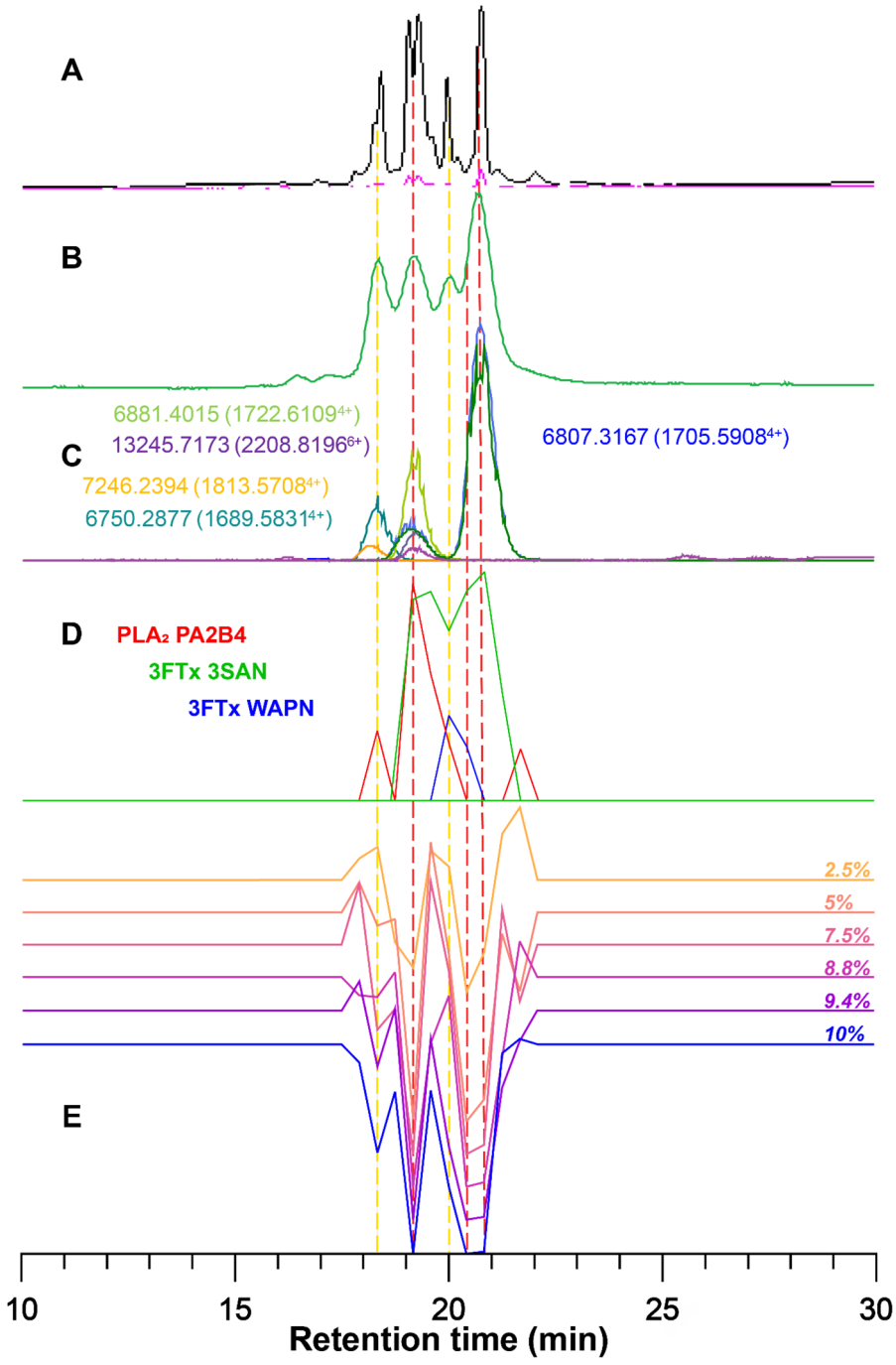

Figure 7. Identification of toxins in nanofractionated *N. nigricollis* venom by correlating LC-UV data, LC-MS data, HT venomics data, and chromatographic *in vivo* bioactivity data (i.e. average LI). Dashed lines showing the significantly bioactive fractions (yellow: paralytic; red: tissue-toxic) (A) LC-UV trace of separated snake venom at 220 nm. (B) Total Ion Current (TIC) of the LC-MS data. (C) Extracted Ion currents (EICs) of toxins eluting at or around the same RT as one of the bioactivity peaks observed. (D) HT venomics data plotted as PSCs of toxins eluting at or around the same RT as one or more of the bioactivity peaks observed. (E) Bioactivity chromatograms obtained by plotting RT on the x-axis and average LI of fractions at different dilutions on the y-axis.

and larvae tend to freeze during the light phases, thus making their behavior indistinguishable from the paralyzing effect of the toxins. The dark phase of the LDC always elicits a hyperactivity response under control conditions and therefore is a suitable experimental phase for our tests.

Calculating ratios of the D of exposed fish over the D of negative controls in each trial allowed us to obtain a single data point per fraction for every trial, the locomotion index (LI), a percentage-based metric derived from behavioral data. The LI expresses the average distance moved during dark phases by

venom-exposed larvae as a percentage of movement by untreated controls within the same experimental trial. Thus, the LI is unitless, but inherently normalized to control performance (set at 100%). To define and quantify locomotion-impairing activity in a more standardized toxicological framework, we propose % Inhibition of Locomotion (relative to control) as practical units. This is directly expressed through the LI. For example, an LI of 40% corresponds to 60% inhibition of dark-phase locomotion compared to the baseline. This novel parameter for locomotion effects led to more accurate measurements by considering the groups of larvae in each trial separately, accounting for the factors affecting the subjects as a group in each multi-well plate, such as handling, time of experimentation, light exposure, activity level, stress levels, or egg water oxygen concentration. Using dose-response curves (see Figure 5), we derived the effective dilution or concentration at which the venom fraction causes a 50% reduction in LI (i.e. 50% hypoactivity). This value can be expressed in volume/volume (% v/v), the dilution factor of the venom solution used (as in the current setup), or mass/volume (µg/mL), when the exact concentration of active toxin in the well is known or estimated *via* venomics.

Out of the 10 fractions obtained from the crude venom of *N. nigricollis*, 5 showed a significantly lower LI than the baseline (Figure 2). We performed the same experiment at lower concentrations of venom toxins by making dilutions, creating dose-response curves for each toxic fraction (Figure 5). This result shows how the assay not only detects locomotion-altering fractions but is precise enough to profile their dosage-related bioactivity. The fractions which caused severe tissue damage (i.e. D7, B8, and C8) all contain toxins of sequences similar to Naniproin (3FTX 3SAN), a cardiotoxin with cytolytic properties (Nasir et al. 2023). Instead, paralytic toxins F7 and B7 share sequence similarity to basic phospholipase A_2 (PLA_2 PA2B4), a toxin known to have a strong anticoagulant (Stefansson et al. 1989), hemolytic (Condrea et al. 1981), and cardiotoxic activity (Fletcher et al. 1981). More precisely, Fletcher et al. (1981) showed that basic PLA_2 induces paralysis in a rat phrenic nerve-diaphragm preparation, in accordance with our results. Nawaprin (WAPN) did not show any visible pathophysiological symptoms as previously reported by Nair et al. (2007).

Cytotoxins-induced local tissue damage, especially necrosis, are the main medically relevant complications in clinical studies of human envenomation by *N. nigricollis* (Warrell 1976; Iddon et al. 1987; WHO Regional Office for Africa 2010; Rivel et al. 2016). Neurotoxicity from *N. nigricollis* venom has been shown in rats (Ajisebiola et al. 2022) but it is not considered to be a predominant clinical concern in human envenomations by *N. nigricollis*. This might be due to the cytotoxic pathological effects overshadowing the neurotoxic ones in patients, thus making separation and characterization of toxins from crude venoms key to detect hidden clinical symptoms that might play a role in the prognosis of snakebite victims.

During toxicity screenings, blood pooling was observed in the heart of subjects exposed to some fractions (Supporting Information, Fig. S1), although specific haemotoxic symptoms such as haemlolysis could not be assessed; more in-depth research is needed to do so. To investigate the possible cardiotoxicity, the heart rate of the subjects was measured under anesthesia and compared to negative controls. The resulting heart rate of larvae exposed to fraction C7 showed a significant bradycardia when compared to the control group (Figure 3), possibly caused by cardiotoxin Naniproin and basic PLA_2. Indeed, basic PLA_2 can affect the cardiac output by reducing the heart contractile force and rate (Fletcher et al. 1982), which could also explain the blood pooling of fractions F7, C7, and B7. While further testing is needed, these preliminary results are promising and may be a prelude for future development of *in vivo* bioassays for cardiovascular toxicity using zebrafish larvae. Oxygen consumption was significantly increased with fraction Nsi_F7 and Nni_H6 (Figure 4), Indicating a higher metabolic rate, probably to generate enough energy to counteract the toxicity effects of these fractions (Gashkina 2024; Meador et al. 2019; Peng et al. 2024).

Based on the results of toxicity profiling, mainly PLA_2s and 3FTXs were causing a decrease in LI values (Figure 7). Due to the limited resolution of the fractionation after the RPLC separation, toxins with similar hydrophobicity at the pH used for separation closely co-eluted in the same fractions during nanofractionation. As a result, synergism between toxins or one toxin hiding the effects of the other might have occurred (e.g. in fraction D7 the 3FTX tissue-toxicity might have concealed PLA_2 paralytic effects). Thus, for future research on this topic, higher resolution fractionation after separation and orthogonal separation methods can offer full separation of all relevant bioactive toxins, in the effort to obtain pure isolated toxins for *in vivo* bioassaying.

Our study includes several layers of quantitative analysis to validate the proof-of-concept and to measure the bioactivity of individual venom fractions. We developed

and applied a novel metric, the Locomotion Index (LI), which quantitatively compares the locomotor activity of exposed larvae to that of controls, normalized per trial. This provides a standardized, percentage-based measure of effect size. For each toxic fraction identified at 10% concentration, we performed dose-response analyses across a dilution series (2.5%–10% v/v). The resulting curves were fitted using least squares regression. This approach clearly demonstrates quantifiable, concentration-dependent effects on larval locomotion. Beyond locomotion, we quantified physiological parameters, heart rate and oxygen consumption, using well-established protocols and statistical analyses. These complementary metrics confirm the physiological impact of venom fractions Finally, our integration of nanofractionation bioactivity chromatograms with UV, MS, EICs, and PSCs provides quantitative correlation between biochemical identity and biological effect.

The here presented methodology has many potential applications in the field of toxicovenomics. Firstly, it can help reduce and partially replace mammalian models in animal experimentations for toxicology studies in favor of zebrafish larvae as a complementary early stage high-throughput screening model (Gerlai 2014). Since zebrafish larvae under 6 dpf are not classified as experimental animals under EU law, this model allows early-stage screening without the ethical and logistical burdens of rodent testing, making it a valuable triage tool before confirmatory tests in mammalian systems. When applied to specific groups of toxins of which the mechanism of action is known, our locomotion bioassay coupled with nanofractionation analytics becomes a tool to efficiently measure toxin-specific toxicity on locomotion. For instance, the nanofractionation approach allows assessment of individual venom components, thus enabling fine-grained evaluation of how well an antivenom neutralizes specific toxins rather than crude venom alone which represents a limitation in traditional rodent lethality assays. The zebrafish model allows direct comparison of venom effects from different snake species, as demonstrated with *N. nigricollis*, *N. haje*, *N. siamensis*, and *N. subfulva*. This broadens the platform's potential for cross-neutralisation testing, a critical requirement for polyvalent antivenoms. When used to analyze α or β-neurotoxins, this bioassay becomes an α/β-neurotoxicity bioassay, effectively measuring neurotoxic paralytic bioactivity *in vivo*. While hypoactivity might be the main focus, significant hyperactivity can be detected as well, which could be relevant for spasms-inducing toxins such as fasciculins and crotamine (Warrell 2010). By pre-incubating toxic venom fractions with candidate antivenoms and subsequently exposing zebrafish larvae during pre-clinical trials, it is possible to test whether the antivenom prevents or mitigates the expected locomotor impairment. A return of the Locomotion Index (LI) toward control values would indicate neutralizing capacity. The availability of dose-response curves for each toxic fraction provides a quantitative baseline for assessing the extent to which an antivenom shifts the curve toward nontoxic concentrations. Research on toxin interactions such as synergism and auxiliary effects can also benefit from this methodology (Laustsen 2016), and combinations of toxins could be investigated. Importantly, it can be employed in antivenomics for analyzing both crude venoms and purified single toxins to test the effectiveness of antivenoms at neutralizing their symptoms. In particular, many aspects of local tissue damage pathogenesis in snake venoms are not yet understood (Gutiérrez et al. 2018; Bittenbinder et al. 2024), and research in this field could use the here presented methodology as a powerful analytical tool.

Furthermore, the application of this *in vivo* bioassay protocol does not need to be limited to snake venoms or to the nanofractionation process. It can easily be applied to study the effects of molecules of unknown or poorly understood mechanisms on the locomotion response of a free-swimming living vertebrate. In that case, our bioassay should be followed up by other tests, aiming at explaining the mechanisms of action of the molecules inducing locomotion alterations. Regarding our results, the presence of potent cytotoxins in *N. nigricollis* venom is well documented (Conlon et al. 2020; Adamude et al. 2021), and made distinguishing them from other toxins *via* toxicity screenings fundamental, as a fully paralyzed fish and a dead fish due to tissue toxicity provide the same kinematic readouts.

Finally, the capability of this behavioral assay to detect dead larvae makes it a useful and quick screening tool for high-throughput biomedical and pharmaceutical applications. Possible applications include monitoring survival rates of specific diseases, drugs safety screenings, and drugs efficacy in treating lethal conditions. Moreover, research fields studying effects occurring over longer time periods (e.g. sleep, stress, and circadian rhythm research) could also benefit from adopting this bioassay. Although we tested the effect of toxins after one hour of exposure, the protocol could easily be adapted to test bioactivity after or during longer exposure times, up to even days. Because drug screening using the light-dark challenge on zebrafish larvae has received increased attention in the last decade (Basnet et al. 2019; Rosa et al. 2022), we believe our study can help improve this rather young *in vivo* approach to test bioactive compounds.

Acknowledgments

We would like to thank Xiaoyi Zhang for helping with the nanofractionation experiments and Dr Jan de Sonneville for providing the picture of a zebrafish larva.

Authors contributions

Conceptualization: G.C., C.T., J.K.; Data curation: G.C., H.N., H.X.; Formal analysis: G.C., H.N., H.X.; Funding acquisition: C.T., J.K.; Investigation: G.C., H.N., H.X., J.S.; Methodology: G.C., H.N., C.T., J.K.; Project administration: C.T., J.K.; Resources: C.T., J.K.; Software: G.C., H.N.; Supervision: C.T., J.K.; Validation: G.C., H.N.; Visualization: G.C., H.N., H.X.; Writing – original draft: G.C., H.N.; Writing – review & editing: G.C., H.N., H.X., M.K.R., C.T., J.K. All authors have read and agreed to the published version of the manuscript.

Disclosure statement

No potential conflict of interest was reported by the author(s).

Funding

The author(s) reported there is no funding associated with the work featured in this article.

Data availability statement

Data are available upon reasonable request.

References

Adamude FA, Dingwoke EJ, Abubakar MS, Ibrahim S, Mohamed G, Klein A, Sallau AB. 2021. Proteomic analysis of three medically important Nigerian Naja (Naja haje, Naja katiensis and Naja nigricollis) snake venoms. Toxicon. 197:24–32. doi: 10.1016/j.toxicon.2021.03.014.

Ajisebiola BS, Adeniji OB, James AS, Ajayi BO, Adeyi AO. 2022. Naja nigricollis venom altered reproductive and neurological functions via modulation of pro-inflammatory cytokines and oxidative damage in male rats. Metabol Open. 14:100188. doi: 10.1016/j.metop.2022.100188.

Arrahman A, Kazandjian TD, Still KBM, Slagboom J, Somsen GW, Vonk FJ, Casewell NR, Kool J. 2022. A combined bioassay and nanofractionation approach to investigate the anticoagulant toxins of mamba and cobra venoms and their inhibition by varespladib. Toxins. 14(11):736. doi: 10.3390/toxins14110736.

Barber CM, Isbister GK, Hodgson WC. 2013. Alpha neurotoxins. Toxicon. 66:47–58. doi: 10.1016/j.toxicon.2013.01.019.

Basnet RM, Zizioli D, Taweedet S, Finazzi D, Memo M. 2019. Zebrafish larvae as a behavioral model in neuropharmacology. Biomedicines. 7(1):23. doi: 10.3390/BIOMEDICINES7010023.

Bauer B, Mally A, Liedtke D. 2021. Zebrafish embryos and larvae as alternative animal models for toxicity testing. Int J Mol Sci. 22(24):13417. doi: 10.3390/ijms222413417.

Bittenbinder MA, Capinha L, Pereira DDC, Slagboom J, Velde B. v. d, Casewell NR, Jennings P, Kool J, Vonk FJ. 2023. Development of a high-throughput in vitro screening method for the assessment of cell-damaging activities of snake venoms. PLoS Negl Trop Dis. 17(8):e0011564. doi: 10.1371/journal.pntd.0011564.

Bittenbinder MA, van Thiel J, Cardoso FC, Casewell NR, Gutiérrez JM, Kool J, Vonk FJ. 2024. Tissue damaging toxins in snake venoms: mechanisms of action, pathophysiology and treatment strategies. Commun Biol. 7(1):358. doi: 10.1038/s42003-024-06019-6.

Bressan Simonetti R, Santos Marques L, Streit DP, Oberst3 R. 2016. Zebrafish (Danio rerio): Ethics in animal experimentation. J Agric Vet Sci. 9(7):106–110. doi: 10.9790/2380-090701106110.

Bucciarelli GM, Alsalek F, Kats LB, Green DB, Shaffer HB. 2022. Toxic relationships and arms-race coevolution revisited. Annu Rev Anim Biosci. 10(1):63–80. doi: 10.1146/annurev-animal-013120-024716.

Canedo A, Saiki P, Santos AL, da Silva Carneiro K, de Souza AM, Qualhato G, da Silva Brito R, Mello-Andrade F, Rocha TL. 2022. Zebrafish (Danio rerio) meets bioethics: the 10Rs ethical principles in research. Cienc Anim Bras. 23(19):70884. doi: 10.1590/1809-6891V22E-70884.

Carvalho JCT, Keita H, Santana GR, de Souza GC, dos Santos IVF, Amado JRR, Kourouma A, Prada AL, de Oliveira Carvalho H, Silva ML. 2018. Effects of Bothrops alternatus venom in zebrafish: a histopathological study. Inflammopharmacology. 26(1):273–284. doi: 10.1007/s10787-017-0362-z.

Casewell NR, Jackson TNW, Laustsen AH, Sunagar K. 2020. Causes and consequences of snake venom variation. Trends Pharmacol Sci. 41(8):570–581. doi: 10.1016/j.tips.2020.05.006.

Cassar S, Adatto I, Freeman JL, Gamse JT, Iturria I, Lawrence C, Muriana A, Peterson RT, Van Cruchten S, Zon LI. 2020. Use of zebrafish in drug discovery toxicology. Chem Res Toxicol. 33(1):95–118. doi: 10.1021/acs.chemrestox.9b00335.

Champagne DL, Hoefnagels CCM, de Kloet RE, Richardson MK. 2010. Translating rodent behavioral repertoire to zebrafish (Danio rerio): relevance for stress research. Behav Brain Res. 214(2):332–342. doi: 10.1016/j.bbr.2010.06.001.

Chippaux JP. 1998. Snake-bites: appraisal of the global situation. Bull World Health Organ. 76(5):515–524. doi: 10.1086/505866.

Condrea E, Fletcher JE, Rapuano BE, Yang CC, Rosenberg P. 1981. Dissociation of enzymatic activity from lethality and pharmacological properties by carbamylation of lysines in Naja nigricollis and Naja naja atra snake venom phospholipases A2. Toxicon. 19(5):705–720. doi: 10.1016/0041-0101(81)90108-2.

Conlon JM, Attoub S, Musale V, Leprince J, Casewell NR, Sanz L, Calvete JJ. 2020. Isolation and characterization of cytotoxic and insulin-releasing components from the venom of the black-necked spitting cobra Naja nigricollis (Elapidae). Toxicon X. 6:100030. doi: 10.1016/j.toxcx.2020.100030.

Dai YJ, Jia YF, Chen N, Bian WP, Li QK, Ma YB, Chen YL, Pei DS. 2014. Zebrafish as a model system to study toxicology. Environ Toxicol Chem. 33(1):11–17. doi: 10.1002/etc.2406.

Davis R, Luchtenburg F, Richardson M, Schaaf M, Tudorache C, Slabbekoorn H. 2021. The importance of individual variation for the interpretation of behavioural studies: ethanol

effects vary with basal activity level in zebrafish larvae. Psychopharmacology. 238(11):3155–3166. doi: 10.1007/s00213-021-05932-6.

de Esch C, van der Linde H, Slieker R, Willemsen R, Wolterbeek A, Woutersen R, De Groot D. 2012. Locomotor activity assay in zebrafish larvae: influence of age, strain and ethanol. Neurotoxicol Teratol. 34(4):425–433. doi: 10.1016/j.ntt.2012.03.002.

Dutta S, Chanda A, Kalita B, Islam T, Patra A, Mukherjee AK. 2017. Proteomic analysis to unravel the complex venom proteome of eastern India Naja naja: correlation of venom composition with its biochemical and pharmacological properties. J Proteomics. 156:29–39. doi: 10.1016/j.jprot.2016.12.018.

Ellis LD, Seibert J, Soanes KH. 2012. Distinct models of induced hyperactivity in zebrafish larvae. Brain Res. 1449:46–59. doi: 10.1016/j.brainres.2012.02.022.

Emran F, Rihel J, Dowling JE. 2008. A behavioral assay to measure responsiveness of Zebrafish to changes in light intensities. J Vis Exp. 20(20):1–6. doi: 10.3791/923.

Engeszer RE, Patterson LB, Rao AA, Parichy DM. 2007. Zebrafish in the wild: a review of natural history and new notes from the field. Zebrafish. 4(1):21–40. doi: 10.1089/zeb.2006.9997.

Faught E, Vijayan MM. 2022. Coordinated action of corticotropin-releasing hormone and cortisol shapes the acute stress-induced behavioural response in zebrafish. Neuroendocrinology. 112(1):74–87. doi: 10.1159/000514778.

Fletcher JE, Rapuano BE, Condrea E, Yang CC, Rosenberg P. 1981. Relationship between catalysis and toxicological properties of three phospholipases A2 from elapid snake venoms. Toxicol Appl Pharmacol. 59(2):375–388. doi: 10.1016/0041-008X(81)90209-X.

Fletcher JE, Yang CC, Rosenberg P. 1982. Basic phospholipase A2 from Naja nigricollis snake venom: phospholipid hydrolysis and effects of electrical and contractile activity of the rat heart. Toxicol Appl Pharmacol. 66(1):39–54. doi: 10.1016/0041-008X(82)90059-X.

Gashkina NA. 2024. Metal toxicity: effects on energy metabolism in fish. IJMS. 25(9):5015. doi: 10.3390/ijms25095015.

Gerlai R. 2014. Fish in behavior research: unique tools with a great promise! J Neurosci Methods. 234:54–58. doi: 10.1016/j.jneumeth.2014.04.015.

Grieco F, Tegelenbosch RAJ, Noldus LPJJ. 2020. Software tools for behavioral phenotyping of zebrafish across the life span. In: Gerlai RT, editors. Behavioral and neural genetics of zebrafish. Cambridge (MA): Academic Press. doi: 10.1016/b978-0-12-817528-6.00030-9.

Gutiérrez JM, Calvete JJ, Habib AG, Harrison RA, Williams DJ, Warrell DA. 2017. Snakebite envenoming. Nat Rev Dis Primers. 3(1):17079. doi: 10.1038/NRDP.2017.63.

Gutiérrez JM, Rucavado A, Escalante T, Herrera C, Fernández J, Lomonte B, Fox JW. 2018. Unresolved issues in the understanding of the pathogenesis of local tissue damage induced by snake venoms. Toxicon. 148:123–131. doi: 10.1016/j.toxicon.2018.04.016.

Horzmann KA, Freeman JL. 2018. Making waves: new developments in toxicology with the zebrafish. Toxicol Sci. 163(1):5–12. doi: 10.1093/toxsci/kfy044.

Howe K, Clark MD, Torroja CF, Torrance J, Berthelot C, Muffato M, Collins JE, Humphray S, McLaren K, Matthews L, et al. 2013. The zebrafish reference genome sequence and its relationship to the human genome. Nature. 496(7446):498–503. doi: 10.1038/nature12111.

Iddon D, Theakston RDG, Ownby CL. 1987. A study of the pathogenesis of local skin necrosis induced by Naja nigricollis (spitting cobra) venom using simple histological staining techniques. Toxicon. 25(6):665–672. doi: 10.1016/0041-0101(87)90113-9.

Kasturiratne A, Wickremasinghe AR, De Silva N, Gunawardena NK, Pathmeswaran A, Premaratna R, Savioli L, Lalloo DG, De Silva HJ. 2008. The global burden of snakebite: a literature analysis and modelling based on regional estimates of envenoming and deaths. PLOS Med. 5(11):e218. doi: 10.1371/journal.pmed.0050218.

Laustsen AH. 2016. Toxin synergism in snake venoms. Toxin Reviews. 35(3-4):165–170. doi: 10.1080/15569543.2016.1220397.

Legradi J, el Abdellaoui N, van Pomeren M, Legler J. 2015. Comparability of behavioural assays using zebrafish larvae to assess neurotoxicity. Environ Sci Pollut Res Int. 22(21):16277–16289. doi: 10.1007/s11356-014-3805-8.

Leyden C, Brüggemann T, Debinski F, Simacek CA, Dehmelt FA, Arrenberg AB. 2022. Efficacy of tricaine (MS-222) and hypothermia as anesthetic agents for blocking sensorimotor responses in larval zebrafish. Front Vet Sci. 9:864573. doi: 10.3389/fvets.2022.864573.

Luchtenburg FJ, Schaaf MJM, Richardson MK. 2019. Functional characterization of the cannabinoid receptors 1 and 2 in zebrafish larvae using behavioral analysis. Psychopharmacology. 236(7):2049–2058. doi: 10.1007/s00213-019-05193-4.

Mackessy SP. 2009. The field of reptile toxinology: snakes, lizards, and their venoms. In: Mackessy SP, editor. Handbook of venoms and toxins of reptiles. Boca Raton: CRC Press. p. 3–19.

Meador JP, Nahrgang J. 2019. Characterizing crude oil toxicity to early-life stage fish based on a complex mixture: are we making unsupported assumptions? Environ Sci Technol. 53(19):11080–11092. doi: 10.1021/acs.est.9b02889.

Mladic M, de Waal T, Burggraaff L, Slagboom J, Somsen GW, Niessen WMA, Manjunatha Kini R, Kool J. 2017. Rapid screening and identification of ACE inhibitors in snake venoms using at-line nanofractionation LC-MS. Anal Bioanal Chem. 409(25):5987–5997. doi: 10.1007/s00216-017-0531-3.

Mladic M, Slagboom J, Kool J, Vonk FJ, van Wezel GP, Richardson MK. 2018. Detection and identification of antibacterial proteins in snake venoms using at-line nanofractionation coupled to LC-MS. Toxicon. 155:66–74. doi: 10.1016/j.toxicon.2018.08.009.

Mladic M, Zietek BM, Iyer JK, Hermarij P, Niessen WMA, Somsen GW, Kini RM, Kool J. 2016. At-line nanofractionation with parallel mass spectrometry and bioactivity assessment for the rapid screening of thrombin and factor Xa inhibitors in snake venoms. Toxicon. 110:79–89. doi: 10.1016/j.toxicon.2015.12.008.

Moretz JA, Martins EP, Robison BD. 2007. Behavioral syndromes and the evolution of correlated behavior in zebrafish. Behavioral Ecology. 18(3):556–562. doi: 10.1093/beheco/arm011.

Nair DG, Fry BG, Alewood P, Kumar PP, Kini RM. 2007. Antimicrobial activity of omwaprin, a new member of the waprin family of snake venom proteins. Biochem J. 402(1):93–104. doi: 10.1042/BJ20060318.

Nasir NJM, Heemskerk H, Jenkins J, Hamadee NH, Bunte R, Tucker-Kellogg L. 2023. Myoglobin-derived iron causes wound enlargement and impaired regeneration in pressure injuries of muscle. Elife. 12:1–34. doi: 10.7554/eLife.85633.

Neumann C, Slagboom J, Somsen GW, Vonk F, Casewell NR, Cardoso CL, Kool J. 2020. Development of a generic high-throughput screening assay for profiling snake venom protease activity after high-resolution chromatographic fractionation. Toxicon. 178:61–68. doi: 10.1016/j.toxicon.2020.02.015.

Otvos RA, Mladic M, Arias-Alpizar G, Niessen WMA, Somsen GW, Smit AB, Kool J. 2016. At-Line cellular screening methodology for bioactives in mixtures targeting the α7-nicotinic acetylcholine receptor. J Biomol Screen. 21(5):459–467. doi: 10.1177/1087057115625307.

Peng X, Lin J, Zhu Y, Liu X, Zhang Y, Ji Y, Yang X, Zhang Y, Guo N, Li Q. 2016. Anxiety-related behavioral responses of pentylenetetrazole-treated zebrafish larvae to light-dark transitions. Pharmacol Biochem Behav. 145:55–65. doi: 10.1016/j.pbb.2016.03.010.

Peng Y, He Q. 2024. Reproductive toxicity and related mechanisms of micro(nano)plastics in terrestrial mammals: review of current evidence. Ecotoxicol Environ Saf. 279:116505. doi: 10.1016/j.ecoenv.2024.116505.

Peterson RT, MacRae CA. 2012. Systematic approaches to toxicology in the zebrafish. Annu Rev Pharmacol Toxicol. 52(1): 433–453. doi: 10.1146/annurev-pharmtox-010611-134751.

Pungerčar J, Križaj I. 2007. Understanding the molecular mechanism underlying the presynaptic toxicity of secreted phospholipases A2. Toxicon. 50(7):871–892. doi: 10.1016/j.toxicon.2007.07.025.

R Core Team. 2022. *R: a language and environment for statistical computing*. R Foundation for Statistical Computing. https://www.r-project.org/.

Ranawaka UK, Lalloo DG, de Silva HJ. 2013. Neurotoxicity in snakebite-the limits of our knowledge. PLOS Negl Trop Dis. 7(10):e2302. doi: 10.1371/journal.pntd.0002302.

Rivel M, Solano D, Herrera M, Vargas M, Villalta M, Segura Á, Arias AS, León G, Gutiérrez JM. 2016. Pathogenesis of dermonecrosis induced by venom of the spitting cobra, Naja nigricollis: an experimental study in mice. Toxicon. 119:171–179. doi: 10.1016/j.toxicon.2016.06.006.

Rock S, Rodenburg F, Schaaf MJM, Tudorache C. 2022. Detailed analysis of zebrafish larval behaviour in the light dark challenge assay shows that diel hatching time determines individual variation. Front Physiol. 13:827282. doi: 10.3389/fphys.2022.827282.

Rosa JGS, Lima C, Lopes-Ferreira M. 2022. Zebrafish larvae behavior models as a tool for drug screenings and pre-clinical trials: a review. Int J Mol Sci. 23(12):6647. doi: 10.3390/ijms23126647.

RStudio Team. 2022. *RStudio: integrated development environment for R*. RStudio, PBC. http://www.rstudio.com/.

Sahyoun C, Krezel W, Mattei C, Sabatier J-M, Legros C, Fajloun Z, Rima M. 2022. Neuro- and cardiovascular activities of *Montivipera bornmuelleri* snake venom. Biology. 11(6):888. doi: 10.3390/biology11060888.

Slagboom J, Derks RJE, Sadighi R, Somsen GW, Ulens C, Casewell NR, Kool J. 2023. High-throughput venomics. J Proteome Res. 22(6):1734–1746. doi: 10.1021/acs.jproteome.2c00780.

Slagboom J, Mladić M, Xie C, Kazandjian TD, Vonk F, Somsen GW, Casewell NR, Kool J. 2020. High throughput screening and identification of coagulopathic snake venom proteins and peptides using nanofractionation and proteomics approaches. PLOS Negl Trop Dis. 14(4):e0007802. doi: 10.1371/journal.pntd.0007802.

Steenbergen PJ, Richardson MK, Champagne DL. 2011. The use of the zebrafish model in stress research. Prog Neuropsychopharmacol Biol Psychiatry. 35(6):1432–1451. doi: 10.1016/j.pnpbp.2010.10.010.

Stefansson S, Kini RM, Evans HJ. 1989. The inhibition of clotting complexes of the extrinsic coagulation cascade by the phospholipase A2 isoenzymes from Naja nigricollis venom. Thromb Res. 55(4):481–491. doi: 10.1016/0049-3848(89)90056-X.

Still KBM, Nandlal RSS, Slagboom J, Somsen GW, Casewell NR, Kool J. 2017. Multipurpose HTS coagulation analysis: assay development and assessment of coagulopathic snake venoms. Toxins. 9(12):382. doi: 10.3390/toxins9120382.

Still KBM, Slagboom J, Kidwai S, Xie C, Zhao Y, Eisses B, Jiang Z, Vonk FJ, Somsen GW, Casewell NR, et al. 2020. Development of high-throughput screening assays for profiling snake venom phospholipase A2 activity after chromatographic fractionation. Toxicon. 184:28–38. doi: 10.1016/j.toxicon.2020.05.022.

Tal T, Yaghoobi B, Lein PJ. 2020. Translational toxicology in zebrafish. Curr Opin Toxicol. 23-24:56–66. doi: 10.1016/j.cotox.2020.05.004.

Tasoulis T, Isbister GK. 2017. A review and database of snake venom proteomes. Toxins (Basel). 9(9):290. doi: 10.3390/toxins9090290.

Tudorache C, Ter Braake A, Tromp M, Slabbekoorn H, Schaaf MJM. 2015. Behavioral and physiological indicators of stress coping styles in larval zebrafish. Stress. 18(1):121–128. doi: 10.3109/10253890.2014.989205.

van Thiel J, Khan MA, Wouters RM, Harris RJ, Casewell NR, Fry BG, Kini RM, Mackessy SP, Vonk FJ, Wüster W, et al. 2022. Convergent evolution of toxin resistance in animals. Biol Rev Camb Philos Soc. 97(5):1823–1843. doi: 10.1111/brv.12865.

Vargas RA, Sarmiento K, Vásquez IC. 2015. Zebrafish (Danio rerio): A Potential Model for Toxinological Studies. Zebrafish. 12(5):320–326. doi: 10.1089/zeb.2015.1102.

Warrell DA. 1976. Necrosis, haemorrhage and complement depletion. Q J Med. 45(177):1–22.

Warrell DA. 2010. Snake bite. Lancet. 375(9708):77–88. doi: 10.1016/S0140-6736(09)61754-2.

WHO Regional Office for Africa. 2010. Guidelines for the prevention and clinical management of snakebite in Africa. WHO Regional Office for Africa, 1–145. https://apps.who.int/iris/handle/10665/204458.

Wong RY, Perrin F, Oxendine SE, Kezios ZD, Sawyer S, Zhou L, Dereje S, Godwin J. 2012. Comparing behavioral responses across multiple assays of stress and anxiety in zebrafish (Danio rerio). Behav. 149(10-12):1205–1240. doi: 10.1163/1568539X-00003018.

World Health Organization. 2018. Global snakebite burden. WHO report EB142/17 (2018). doi: 10.1038/nrdp.2017.63.1.

Xie C, Bittenbinder MA, Slagboom J, Arrahman A, Bruijns S, Somsen GW, Vonk FJ, Casewell NR, García-Vallejo JJ, Kool J. 2021. Erythrocyte haemotoxicity profiling of snake venom toxins after nanofractionation. J Chromatogr B Analyt Technol Biomed Life Sci. 1176:122586. doi: 10.1016/j.jchromb.2021.122586.

Xie C, Slagboom J, Albulescu LO, Bruyneel B, Still KBM, Vonk FJ, Somsen GW, Casewell NR, Kool J. 2020. Antivenom neutralization of coagulopathic snake venom toxins assessed by bioactivity profiling using nanofractionation analytics. Toxins. 12(1):53. doi: 10.3390/toxins12010053.

Zanotty Y, Álvarez M, Perdomo L, Sánchez EE, Giron ME, Jimenez JC, Suntravat M, Guerrero B, Ibarra C, Montero Y, et al. 2019. Mutacytin-1, a new C-type lectin-like protein from the venezuelan cuaima (Lachesis muta muta Linnaeus, 1766) (serpentes: viperidae) snake venom inducing cardiotoxicity in developing zebrafish (Danio rerio) embryos. Zebrafish. 16(4):379–387. doi: 10.1089/zeb.2019.1731.

Zietek BM, Mayar M, Slagboom J, Bruyneel B, Vonk FJ, Somsen GW, Casewell NR, Kool J. 2018. Liquid chromatographic nanofractionation with parallel mass spectrometric detection for the screening of plasmin inhibitors and (metallo)proteinases in snake venoms. Anal Bioanal Chem. 410(23):5751–5763. doi: 10.1007/s00216-018-1253-x.